J. Vincenc Oboňa, V. Ocelík, B. Visser, J.Th.M. De Hosson, J.Z.P. Skolski, V.S. Mitko, G.R.B.E. Römer, A.J. Huis in `t Veld. Stainless steel surface modified by ultra short laser pulses, Proceedings of the 24th International Conference on, SURFACE MODIFICATION TECHNOLOGIES (SMT 24), September 7 - 9, 2010 in Dresden, Germany.

Microscopy study of ripples created on steel surface by use of ultra short laser pulses

J. Vincenc Oboňa[1,*,a], V. Ocelík[1], B. Visser[1], J.Th.M. De Hosson[1], J.Z.P. Skolski[2], V.S. Mitko[2], G.R.B.E. Römer[2], A.J. Huis in `t Veld[2,3]

[1] *Department of Applied Physics, Materials innovation institute (M2i), University Groningen, Nijenborgh 4, 9747 AG, The Netherlands*
[2] *University of Twente, Faculty of Engineering Technology and Materials innovation institute, P.O. Box 217, 7500 AE, Enschede, the Netherlands*
[3] *TNO Science & Industry, Department Materials Technology, De Rondom 1, 5600 HE, Eindhoven, The Netherlands*

Abstract

This paper concentrates on ripples on the surface of steel that arise from laser-material interaction.

In particular we have observed two different sets of ripples on steel samples that were machined by 210 fs laser pulses with 800 nm wavelength at normal incidence. Small ripples were found with spacing of about 250 nm lying longitudinal to the vector of laser beam polarization. Big ripples exhibited at a much larger distance of about 500 nm and they are perpendicular to the polarization vector. The laser treated surfaces were investigated with Scanning Electron, Confocal and Atomic Force Microscopy.

The laser-material interaction could be divided into three subsequent steps: absorption of laser light via electron gas excitations, transfer of heat into the lattice followed by a thermal expansion of material. From our microscopic observations it is concluded that the small ripples are formed by solidification of liquid material present as a thin layer near the interface of solid bulk material.

Key words: fs laser pulses, ripples, Scanning Electron Microscopy, Confocal Microscopy, Atomic Force Microscopy

1. Introduction

The ripple structures at the surface, which arise from laser-material interaction with ulra short laser pulses, offer new possibilities for mass industrial production of functional surfaces based on features in 100 nm - 10 µm range.

In depth understanding of the ultrashort pulse Laser-Matter Interaction (LMI) is still lacking although the subject has been under investigation over past 45 years [1]. The LMI modifies a sample surface in such a way that periodic structures, so-called ripples, also known as Laser Induced Periodic Surface Structures (LIPSS), appear after the ultrashort pulse impingement. Several theoretical models have been proposed to predict the characteristic length scales of those ripples [1,2,3].

The most appreciated theoretical model as proposed by Sipe and Young [4] has the virtue to explain the surface features observed after LMI using a electromagnetic approach within the framework of the so-called efficacy factor theory. They explained the LMI as a modulation of energy input into a sample surface caused by the interference of the laser beam

[*] **Corresponding author. Tel: +31 (0)50 363 4890; fax: +31 (0) 50 363 4881; e-mail: j.vincenc.obona@rug.nl**
[a] **On leave from Institute of Electrical Engineering, Slovak Academy of Sciences, Dúbravská Cesta 9, 841 01 Bratislava, Slovak Republic.**

acting on the sample surface with the wave scattered on a so-called selvedge region (surface roughness). The ripples created are either transverse or longitudinal to the polarization vector with a periodicity deduced from the wavelength of the laser light, angle of the laser beam incidence, duration of the laser pulse and refraction index of the treated material.

The objective of this article is to study topography of steel surfaces modified by ultra-short laser pulses on the femtosecond time scale. Detailed inspection by Scanning Electron Microscopy (SEM), Confocal Microscopy (CM) and Atomic Force Microscopy (AFM) has been done. The SEM observation that indicates the presence of liquid state has led us to suggestions about possible mechanisms of melting during LMI.

2 Experimental Details

2.1 Femto-second laser pulses on high temperature alloyed steel 800H

A titanium sapphire based laser system with a central wavelength of 800 nm was used for generation of 210 fs laser pulses with a Gaussian energy distribution. The system delivers the pulses with frequency of 50 kHz. Average powers of 5, 10, 25 and 30 mW were applied, respectively. The experiments were performed by irradiation the material in parallel line sets with various conditions.

Laser beam scanning speed varied from 50, 100, 200, 400, to 800 mm/s. To study the effect of multiple energy delivery 2, 5, 10 and 20 overscans were employed. The diameter of the laser beam spot was not perfectly circular with major axis ~ 24 µm and minor axis ~ 17 µm. High temperature 800H steel was used as a substrate. Chemical composition of the 800H steel is listed in Table 1. The surface was chemically etched to highlight grain boundaries on the surface. More details concerning this experiment are found elsewhere [5].

Table 1: Chemical composition of 800H steel substrate

	C	Cr	Fe	Ni	Al	Ti	Al/Ti
	weight %						
800H	0.06-0.1	19.0-23.0	bulk	30.0-35.0	0.15-0.6	0.15-0.6	0.85-1.2

2.2 Analyses of the surfaces

Three different microscopy techniques were applied to investigate the sample surfaces treated by ultrashort laser pulses. The Philips XL30 SEM equipped with field emission gun offers lateral resolution of the surface objects at few nanometers level. Height information of the surface features was obtained by AFM measurements with a resolution depending on the AFM stylus tip radius of about 20 nm. Amount of the ablated material inside laser tracks was measured by optical Confocal Microscope (CM) µSurf Nanofocus, observing their depth profiles.

3 Results

3.1 SEM observations

Scanning electron microscopy observations were performed on the 800H steel sample treated by 210 fs laser pulses in order to investigate shape and direction evolution of the ripples in dependence on delivered fluence. Fig.1. shows the area that absorbed the very last few laser pulses from the in total 500 µm long laser processed track. Combination of the scanning speed and the repetition rate of the laser machining results in a distance between subsequent pulses of 1 µm in this case. "Fingerprint" of the last laser pulse covers around 5/6 of the picture (from left) and number of the overlapped pulses within the displayed view is about 14. The Gaussian energy distribution permits to calculate the fluence distribution map in the single pulse as well as in the track with the maxima being approximately 0.35 Jcm^{-2} and 4 Jcm^{-2}, respectively.

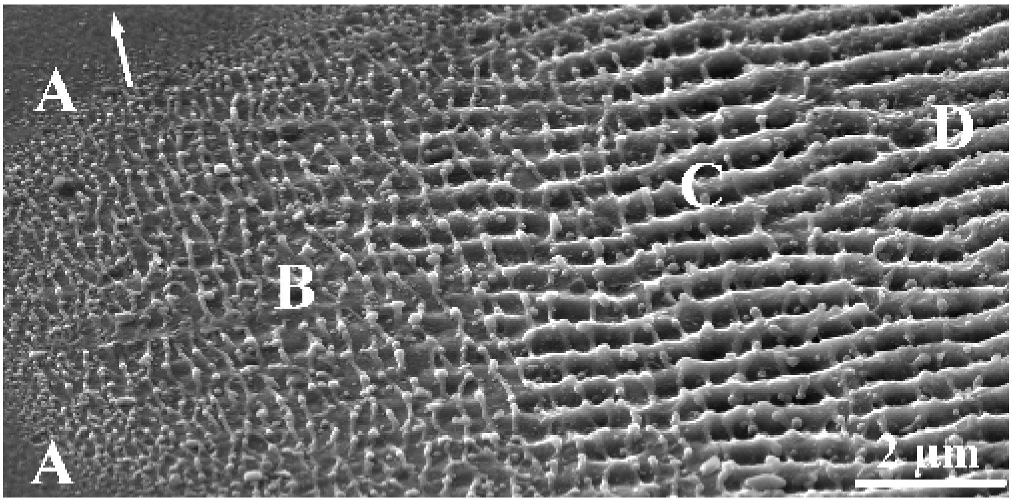

Fig. 1 The end of the track illuminated by a few last pulses from the whole 500 µm long laser track (horizontal to the SEM picture, machined from right to left) which was created by 30 mW average laser power. Repetition rate of 50 kHz and machining speed of 50 mm/s results in 1 µm distance between subsequent pulses. The view is 55° inclined from normal to the sample surface. The beam polarization vector is marked by arrow.

The surface features change continuously upon increasing the fluence. Near the edge of the laser track A at the lowest fluence, due to the Gaussian energy distribution, depressions are found (left-bottom and left-up corner of the Fig.1) and also rounded protrusions at slightly higher energy. As the fluence is progressively increasing, the protrusions started to be organized into aligned linear elongated objects - small ripples - with ragged top edges B (left third of the picture). The small ripples are parallel to the laser polarization. In the region of the steepest increase of fluence C, the surface becomes a mixture of small and big ripples where the small ripples cross the big ones. At the highest fluence area D, almost all small ripples lie at the bottom of valleys between big ripples being always perpendicular to big ripples walls. At highest fluence the big ripples are often discontinued and therefore small ripples at these places become oriented independently on the polarization direction. The globular objects created at a lower fluence level and the small ripples suggest the presence of a liquid matter on the sample surface during the laser matter interaction.

3.2 Confocal Microscopy

Confocal microscopy was used to evaluate the dependence of laser tracks depth on applied laser beam fluence (Fig. 2). The graph shows this dependence for different average laser powers. It clearly demonstrates the linear character of the dependence independently whether the fluence was achieved by overlapping of laser spots or by overscanning of the laser tracks. So, it is controlled not by fluence but ‘cumulated’ fluence. The speed of surface material removal is the highest for the smallest laser power 5 mW and it is almost the same for two of the highest laser powers applied. This dependency of laser track depth on the fluence will be discussed later.

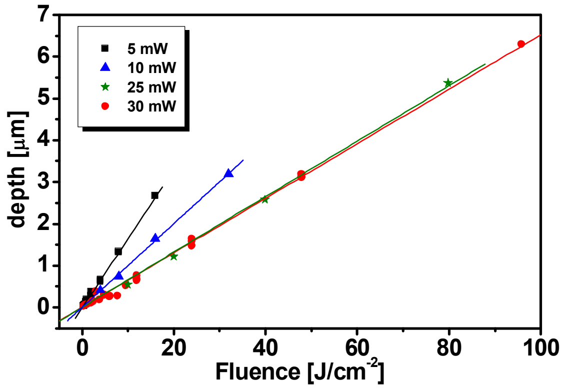

Fig. 2: Graph of the laser tracks depth dependence on used fluence. The four lines belong to four different laser average powers 5, 10, 25 and 30 mW.

3.3 Atomic force microscopy

The AFM method supplemented height information to the SEM analysis. In the experiment, we scanned matrix of 25 laser generated tracks prepared at 30 mW average laser power, at five different machining speeds and at five different number of overscans.

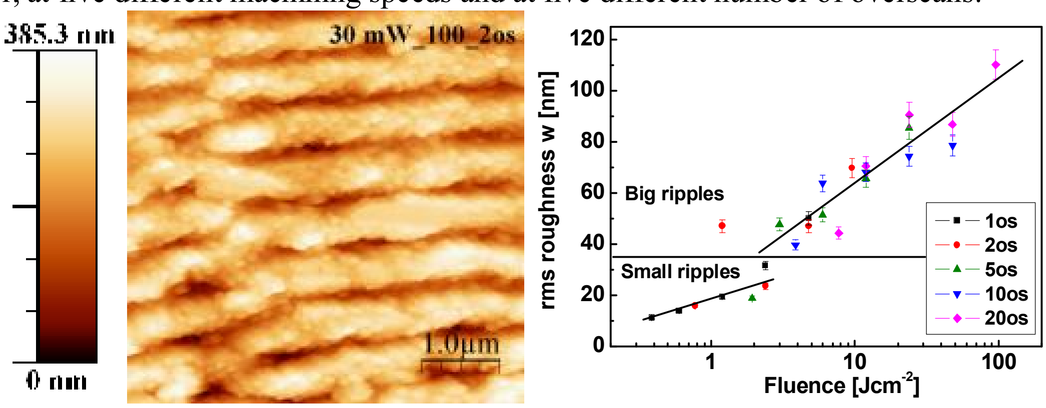

Fig. 3: Example of AFM scan performed on the laser treated sample at 30 mW laser pulse power, 100 mm/s machining velocity and 2 overscans. The right graph of RMS roughness dependence on the used fluence shows 25 values in different colours according number of overscans. The graph is divided into two regions corresponding to small and big ripples induced roughness.

The WSxM Scanning Probe Microscopy software was used for evaluation of the scans in order to find roughness characteristics of the surface features. The Fig. 3 shows 2D representation of 3D scan of the laser track as well as overall graph of the root mean square (RMS) roughness dependence on used fluence for 30 mW laser pulse power.

4 Discussion

In literature, it is assumed that pulses with duration shorter than a few picoseconds do not lead to liquid state formation [6]. The ablation is considered as a quick and direct solid-vapor or solid-plasma transition where heat transport into a target can be neglected [6]. However, Koch et al. [7] indicated the presence of liquid state at the surface even after 100 and 30 fs laser pulses. A process called 'non thermal melting' is mentioned in [8] when at time scale of 100 fs the disordering of the lattice should occur faster than lattice heating. As mentioned above, we also observed clear evidences of the liquid phase presence for 210 fs laser pulses over a broad range of laser power and fluencies on steel samples. Many features on the surface observed by SEM (Fig. 1) suggest rounding of the surface features by the surface tension during the resolidification. The most important part of the interaction, from viewpoint of liquid phase presence explanation, is time needed for the delivery of energy from overheated electron gas into phonons. Short time of the transport favours direct solid-gas ablation whereas much slower cooling of electrons results in creation of a liquid phase.

In the case that the fluence is over the ablation threshold, material in the laser tracks starts to be removed. We found a linear relationship between the applied fluence and the depth of the tracks by CM (Fig. 2). Moreover, we found a dip in the ablation rate with increasing average laser power. The larger laser power, the larger amount of ablated material in LMI zone. If time between two subsequent pulses for multiple-pulse process is short (20 μs in the experiment-repetition rate 50 kHz), it can significantly influence the amount of delivered beam energy to the sample surface as the laser pulse is shielded by ejected material of the previous pulse.

The last microscopy technique used for investigation of the laser treated sample surface was the AFM. AFM cantilever stylus allows us to measure the 3D surface profiles with approximately 20 nm resolution (Fig.3 - left). The measurements were performed in the centre of longitudinal axis of the tracks. We found by use of the WSxM software the maximum height of the small and the big ripples ranging between 60 nm and 250 nm, respectively. A statistical approach to investigate the surface roughness has also been used. The RMS roughness represents 68 % of the ripples heights smaller than 2σ according a Gaussian distribution of the surface roughness. In the graph, we can clearly recognize two regions where two different slopes of the RMS-fluence dependence were measured. The value smaller than 35 nm belong to RMS roughness of the small ripples whereas the values larger that the threshold limit represents the big ripples RMS roughness.

5 Conclusion

Three microscopy techniques were used to study the topography of the 800H steel surface after its treatment by 210 fs laser pulses with repetition rate of 50 kHz and power of 5, 10, 25 and 30 mW.

- Evolution of the surface objects created by laser pulses at low fluence starts with the formation of small spherical objects followed at increasing fluence with elongated small ripples parallel to laser beam polarization vector. Small ripples, oriented parallel to the

polarization of the laser beam are typical for areas treated by low fluencies. These objects have a characteristic height of 30-60 nm and distance between them of 100-250 nm.
- With increasing the fluence, the mixture of small and big ripples, perpendicular to each other, appears. Big ripples are typically 100-400 nm in height and 500 nm distant from each other.
- At the highest cumulated fluence the direction of small ripples become independent on the polarization. Simultaneously, they lie at the bottom of the valleys between the big ripples.
- At all levels of fluence the surface features suggest the presence of a liquid phase during or after the laser pulse.
- Confocal microscopy shows a linear dependence of laser track depth on used fluence. A dip in the ablation rate with increasing laser power suggests a shielding effect due to a larger amount of ejected material over the sample surface.
- Atomic Force Microscopy ekes the SEM topography with height information of the surface objects. It shows linear dependence of the ripples height. There is a possibility of clear distinction of small and big ripples dominance at low and high fluence, respectively.

The experimental results stimulate a further deeper understanding of LMI. It is necessary to look at the process as a sequence of following events: energy redistribution on the sample surface via interference, absorption of photons energy by means of electron gas excitations followed by a transport of this energy into phonons and the final response of irradiated material.

Acknowledgements

This research was carried out under Project number M61.3.08300 in the framework of the Research Program of the Materials innovation institute M2i (www.m2i.nl).

References

[1] M. Birnbaum, "Semiconductor surface damage produced by ruby lasers", *Journal of Applied Physics* **36**, Issue 11, (1965) 3688.
[2] M Ali, T. Wagner, M. Shakoor, P. Molian, "Review of laser nanomachining", *J. of Laser Appl.* **20**, Issue 3, (2008) 169.
[3] J. Reif, F. Costache, M. Bestehorn, Self-Organized Surface Nano-Structuring by Femtosecond Laser Processing, in: Recent Advances in Laser Processing of Materials, Jacques Perriere, Eric Millon, Eric Fogarassy (eds), Elsevier 2006, pp.275-290.
[4] J. E. Sipe, J. F. Young, J. S. Preston, and H. M. van Driel, "Laser-induced periodic surface-structure .1. Theory", *Physical Review B* **27**, Issue 2, (1983)1141.
[5] A. J. Huis in `t Veld and H. van der Veer, "Initiation of Femtosecond Laser Machined Ripples in Steel Observed by Scanning Helium Ion Microscopy (SHIM)", *JLMN-Journal of Laser Micro/Nanoengineering* **5**, Issue 1, (2010) 28.
[6] B. N. Chichkov, C. Momma, S. Nolte, F. von Alvensleben and A. Tünnermann, "Femtosecond, picosecond and nanosecond laser ablation of solids", *Appl. Phys. A* **63**, Issuea 2, (1996) 109.
[7] J. Koch, F. Forte, T. Bauer, C. Fallnich, A. Ostendorf and B. N. Chichkov, "Nanotexturing of gold films by femtosecond laser-induced melt dynamics", *Appl. Phys. A* **81**, Issue 2, (2005) 325.
[8] B. Rethfeld, K. Sokolowski-Tinten, D. von der Linde, S.I. Anisimov, Timescales in the response of materials to femtosecond laser excitation, *Appl. Phys. A* 79, Issue 4-6, (2004) 767.